Viability of the Method of Characteristics for unsteady, non-isothermal, real gas analysis in piping networks

14th International Conference on Pressure Surges
April 12-14, 2023 | Eindoven, Netherlands | Copyright© TU Eindhoven

Scott A. Lang P.E.
Applied Flow Technology
Colorado Springs, Colorado, USA

Mark A. Dudley
Applied Flow Technology
Colorado Springs, Colorado, USA

Viability of the Method of Characteristics for unsteady, non-isothermal, real gas analysis in piping networks

S A Lang, M A Dudley
Applied Flow Technology, USA

ABSTRACT

The Method of Characteristics is widely preferred for analyzing unsteady liquid networks, in part due to the straightforward modeling of complex inline equipment. More general analyses, including unsteady gas flow, tend to favor Finite Volume formulations due to their conservative nature. These solvers are comparatively complex, making their implementation and use more challenging. Advantages and disadvantages of each method for the analysis of gas networks are discussed here. The Method of Characteristics has limitations, but it is shown here to be a technique worthy of consideration for typical engineering analyses.

1 INTRODUCTION

1.1 Motivation

Accurate numerical modeling of large piping networks is often critical to ensuring their optimal and safe operation. Many such techniques are established for liquid systems [1] [2], but tools for compressible gas are both rarer and more complex [3] [4] [5].

Steady analysis of compressible systems is common, while analysis of acoustic transients in large compressible flow piping networks appears to be an uncommon practice. Problematic situations are often either unaddressed (putting the system at risk) or avoided (via expensive overdesign), which may be due to a lack of knowledge that unchecked compressible surge can pose serious risk to the integrity and safety of the system. Designers or operators may be unaware of practical tools to analyze gas surge and thus resort to simple empirical rules, unclear codes and standards, or overbuilt systems [6].

Consequently, it is desired to develop a tool that allows for *practical analysis* of unsteady compressible flow for piping networks. It is argued here that some amount of error in results is acceptable if the tool allows for both ease of use and straightforward development of complex devices, especially when the usual alternative is no analysis whatsoever.

1.2 Accuracy and practicality

In piping network analysis, an engineer rarely seeks an exact answer. Even if one was attainable, piping networks change regularly. Equipment is frequently added, replaced, or removed to mitigate component wear and degradation. Few system analysts will know with certainty the exact specifications of every component in the system. Even with exact numerical solutions, approximation and uncertainty will still creep their way in.

Safety factors or design margins can account for this uncertainty. Because it is impossible to eliminate this uncertainty, it is unproductive to demand perfection in a practical numerical model. Some uncertainty is acceptable, provided the model enables an engineer to make valid and actionable conclusions for the system's design or operation. Given the choice between a very accurate but difficult to use tool, and a less accurate but more accessible tool, many engineers will sacrifice some accuracy for better ease of use and more immediate results.

1.3 Common approaches to simulation

Two general frameworks to solving the non-linear equations of gas flow are discussed here: the Method of Characteristics (MOC), and the Finite Volume Method (FVM). This paper is not intended to be a survey of all methods for unsteady gas analysis, nor is it intended to be a survey of all possible MOC or FVM formulations – only selected approaches for each method are discussed herein.

2 A BRIEF REVIEW OF FUNDAMENTALS

2.1 First principles

Accurate compressible flow solutions must obey conservation of mass (m), momentum (mu), and energy (me). Also needed is an appropriate equation of state.

2.2 Appropriate assumptions and simplifications for piping networks

In a typical network, piping lengths are orders of magnitude larger than piping diameters, and any given pipe has constant diameter. These conditions make non-axial flow effects negligible in most cases, so a one-dimensional analysis is reasonable.

In one dimensional flow, three forces act on the fluid, barring more exotic situations:

- Upstream and downstream pressure forces (pA).
- Gravity (mg).
- Friction, which imparts a shear stress (τ) that opposes flow along the outer surface of the control volume ($\pi D \cdot \delta x$). Determining τ analytically is extremely difficult – it is much more practical to use an empirical relation. Models of varying complexity exist – herein it is assumed the frictional term can be estimated from the conditions at the previous time level, referred to as a quasi-steady friction approximation [7]. The Darcy-Weisbach equation ($dp = -(f\rho u|u| \cdot dx)/2D$) is assumed to apply, meaning that the frictional force can be determined with $F_{friction} = A \cdot dp = -A \cdot dx(f\rho u|u|/2D)$. For later simplicity, we define the value $\mathcal{F} = -f\rho u|u|/2D$.

Heat transfer ($\dot{Q}$) is assumed to be known, or to be a function only of the previous time level. The only work done by the system is assumed to be pressure work ($\dot{W} = \delta(\rho u A)$).

2.3 Conservation

The mass, momentum, and energy conservation laws for one dimension are:

$$\frac{\boldsymbol{D(m)}}{\boldsymbol{Dt}} = \mathbf{0}\,, \qquad \frac{\boldsymbol{D(mu)}}{\boldsymbol{Dt}} = \sum \boldsymbol{F}, \qquad \frac{\boldsymbol{D(me)}}{\boldsymbol{Dt}} = \dot{\boldsymbol{Q}} - \dot{\boldsymbol{W}}\,, \tag{1}$$

where D/Dt represents a *material derivative*, or rate of change within a *material element*. The boundaries of a material element move with the flow field, and the volume is closed to mass transfer. A control volume fixed in space is often simpler – intuitively, one can understand that the flux of some conserved property into or out of a volume corresponds to an increase or decrease in the total conserved property within the volume. For example,

$$\frac{D(m)}{Dt} = 0 \quad \rightarrow \quad \frac{d}{dt}\int \rho\, dV + \int \rho u\, dA = 0\,. \tag{2}$$

With fundamental mathematics, these integral conservation equations can be transformed into differential form *if and only if the flow field is smooth* [8] [9]. To be compact, the matrix form of these equations is presented, with subscripts denoting partial derivatives.

$$\begin{bmatrix} \rho \\ \rho u \\ \rho e \end{bmatrix}_t + \begin{bmatrix} \rho u \\ \rho u^2 + P \\ u(\rho e + P) \end{bmatrix}_x = \begin{bmatrix} 0 \\ \sum F/V \\ \dot{Q}/V \end{bmatrix} \tag{3}$$

This formulation is in *conservation form*: it directly relates temporal rate of change, flux, and source terms, physically capturing the meaning of the conservation laws. When the source terms are zero, these equations reduce to the one-dimensional Euler equations.

2.4 Equation of state

The system of partial differential equations (3) has four unknowns and closure requires an equation of state. We consider two simple options. First, a *calorically perfect gas*, one with constant specific heats, follows the gamma-law equation of state:

$$e = \hat{e} + \frac{u^2}{2} + gz = \frac{P}{\rho(\gamma - 1)} + \frac{u^2}{2} + gz\,. \tag{4}$$

Where γ denotes the ratio of specific heats, c_p/c_v, and $\hat{e}$ is the specific internal energy. Second, it is instructive to consider a case where the flow is *isentropic and isothermal* [8]. In this case, we assert the speed of sound, c, is a constant value, and we can state that changes in density are proportional to changes in pressure.

$$c = \sqrt{\left(\frac{\partial P}{\partial \rho}\right)_s} = \text{const.} \quad \rightarrow \quad d\rho = \frac{1}{c^2} dp \tag{5}$$

2.4.1 Real gas

A real gas deviates from the calorically perfect relation in equation (4), strongly under some conditions. Using an ideal gas equation of state can significantly impact the physical realism of the model [10], so an alternative is desirable. Embedding a two or three parameter equation of state in analytic form into the equations is possible but dramatically complicates the equations and still foregoes some accuracy.

It is therefore desired to use an arbitrary real gas model that cannot be analytically combined with the conservation equations. This is possible if there exists an equation that represents specific energy e in terms of density, velocity, and pressure. Using only fundamental thermodynamic identities [11], it is possible to construct such a relationship:

$$de = \frac{c_p}{\beta \rho c^2} dP + \left(\frac{P}{\rho} - \frac{c_p}{\beta \rho} \right) d\rho + u du + g dz \,. \tag{6}$$

Equation (6) is valid for any fluid, and via combination with equation (3), one algorithm can adapt to an arbitrary equation of state. The arbitrary equation of state can be used to determine the values of the thermodynamic quantities c_p, β, and c for a given pressure and density. Note that this equation effectively linearizes the thermodynamic behavior of the real fluid around the specified pressure and density.

2.4.2 Simplifications for discussion herein

For clarity of discussion, the remainder of this paper will discuss the gamma-law gas (4) for gas flows, and equation (5) for liquid flows. The only source term considered will be the frictional term as described in section 2.2.

3 THE METHOD OF CHARACTERISTICS

3.1 Overview

Hyperbolic systems represent wave-like phenomena – disturbances propagate through the domain at a finite speed along *characteristics*. While the general behavior is described by a coupled system of partial differential equations, the behavior along a characteristic requires only a single ordinary differential equation.

The *method of characteristics* is a mathematical approach to determine these ordinary differential equations. This method can be discretized and applied to a grid of nodes – an overall technique referred to here as the Method of Characteristics (MOC).

3.1.1 Some advantages of the MOC

The MOC is well known for unsteady analysis in liquid full networks, with a wealth of knowledge built up over many decades of research [1] [2]. It is known to be accurate enough for practical purposes, and most modern advancements cover extension to more exotic problems, such as non-Newtonian fluids [12], fluid-structure interaction [13], unsteady friction calculations [14], or computational improvements [15].

The decomposition of the problem into characteristics explicitly tracks physical waves in the solution, maintaining sharp wavefronts, which is highly desirable for acoustic analysis. Additionally, the problem can be represented by simple and explicit linear compatibility equations which are easily applied to boundaries of potentially complex nature, and readily extend to modeling complex phenomena such as transient forces or cavitation [1].

3.1.2 Some disadvantages of the MOC

The traditional MOC is not conservative – even for liquid flow. For a purist, this alone may fully disbar the method from consideration. But its widespread practical use clearly indicates that non-conservative does not mean untrustworthy.

The standard MOC formulation for liquid flow relies on critical assumptions that have negligible effect on accuracy in typical systems. These assumptions are invalid for gas flow, so extending the MOC to compressible flow entails more significant estimations, which increase uncertainty. Because of the strongly non-linear behavior of unsteady gas dynamics, the MOC suffers from lower accuracy as flow conditions become more extreme. High Mach number flows, or flows exhibiting strong shocks, see notably uncertain predictions.

3.2 Liquid flow

3.2.1 The hyperbolic system

Liquid analysis generally uses the equation of state described by (5), which eliminates the need for the energy conservation equation entirely. We further assert that bulk velocity u is negligible compared to the sonic velocity c, and therefore the advective terms uu_x and $u\rho_x$ (see equation (11)) are negligible. Under these conditions, and the assumptions noted in section 2.4.2, equation (3) can be manipulated algebraically into the nonconservative, primitive form, quasilinear hyperbolic system:

$$\begin{bmatrix} u \\ p \end{bmatrix}_t + \begin{bmatrix} 0 & 1/\rho \\ \rho c^2 & 0 \end{bmatrix} \begin{bmatrix} u \\ p \end{bmatrix}_x = \begin{bmatrix} \mathcal{F}/\rho \\ 0 \end{bmatrix} . \tag{7}$$

The eigenvalues of the matrix in equation (7) are $\lambda = \pm c$, which dictate the characteristic speeds of the system. One can also calculate the corresponding left eigenvectors of the matrix as $l = [\pm \rho c \quad 1]$. Combining the eigenvectors with equation (7) results in the decoupled ordinary differential equations:

$$dp \pm \rho c \cdot du = \pm c\mathcal{F} \quad on \quad dx/dt = \pm c \,. \tag{8}$$

These two ordinary differential equations describe the *acoustic characteristics* present in liquid flow. They are symmetric due to their slopes (dx/dt) differing only in sign.

3.2.2 Integration

Integrating the left-hand side of (8) is trivial as both density and sonic velocity are assumed fixed for liquid analysis. The integral on the right is more interesting – the velocity u embedded in $\mathcal{F}$ (see section 2.2) changes in time. Because the time behavior of u is unknown, the integral must be evaluated with an assumed behavior. Typically, this is done with a geometric mean [16], making the result implicit. To simplify the comparison between liquid and gas flow, the left Reimann sum is taken, giving the fully explicit result:

$$\Delta p \pm \rho c \cdot \Delta u = \pm c\mathcal{F} \cdot \Delta t \qquad on \qquad dx/dt = \pm c\,. \tag{9}$$

Manipulation of (9) gives *compatibility equations* (10) wherein the bracketed quantities are constants for a given calculation. The existence of two unknowns and two equations provides a direct solution for the new values of pressure and velocity.

$$p_{new} = \underbrace{[p \pm c\mathcal{F} \cdot \Delta t \pm \rho c u]}_{C^{\pm}} \mp \underbrace{[\rho c]}_{B^{\pm}} u_{new} \qquad on \quad \frac{dx}{dt} = \pm c \tag{10}$$

3.2.3 Discrete solution

The compatibility equations (10) are applicable at any location. For solutions in a finite length pipe, they are solved at equally spaced discrete nodes. The characteristic velocities, $\pm c$, naturally generate a rectangular grid of nodes in the x, t-plane (Figure 1a).

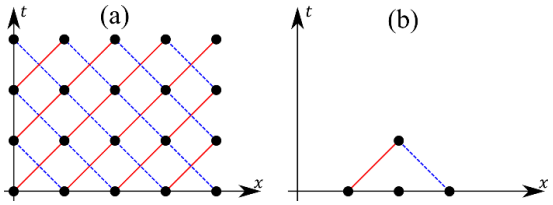

Figure 1: (a) A rectangular grid (b) An independent solution

Solutions at each timestep are computed independently at every node (Figure 1b). To maintain the grid structure, pipe length or sonic velocity must be varied artificially [1].

3.2.4 General junctions and boundary conditions

The availability of the linear and explicit compatibility equations makes the handling of inline junctions and boundary conditions straightforward. For example, a centrifugal pump between two constant diameter pipes might operate on a curve $\Delta p_{new} = 100 - u_{new}^2$. Equation (10) can be arranged to determine $\Delta p_{new} = (C^- + B^-)u_{new} - (C^+ - B^+)u_{new}$, and the pair of equations can be solved directly for u_{new}. More complex arrangements are still relatively easy to compute, perhaps by iterative routines.

3.2.5 Conservation

Looking at the mass conservation equation in (3), it is immediately apparent that for a constant density assumption, no change in velocity is possible. Clearly this cannot be the case if there is transient flow, and therefore the MOC for liquid flow is not truly a conservative solution. Even so, it is still the preferred method for network analysis of liquid transients, which implies that strict conservation is not necessary for practical analysis.

It is important to note that, while the MOC does not *enforce* conservation, it also does not *neglect* it. The solution still originates from the fundamental conservation laws.

3.3 Gas flow

3.3.1 The hyperbolic system

Under the conditions specified in section 2.4.2, equations (3) and (4) can be manipulated into the nonconservative, primitive form, quasilinear hyperbolic system:

$$\begin{bmatrix}\rho\\ u\\ p\end{bmatrix}_t + \begin{bmatrix}u & \rho & 0\\ 0 & u & 1/\rho\\ 0 & \rho c^2 & u\end{bmatrix}\begin{bmatrix}\rho\\ u\\ p\end{bmatrix}_x = \begin{bmatrix}0\\ \mathcal{F}/\rho\\ (\gamma-1)u\mathcal{F}\end{bmatrix}. \tag{11}$$

The eigenvalues and left eigenvectors of the matrix in equation (11) are:

$$\lambda_1 = u - c\,, \qquad \lambda_2 = u\,, \qquad \lambda_3 = u + c\,, \tag{12}$$

$$l_1 = [0 \quad -\rho c \quad 1]\,, \qquad l_2 = [1 \quad 0 \quad -1/c^2]\,, \qquad l_3 = [0 \quad \rho c \quad 1]\,. \tag{13}$$

When combined with the system described by equation (11), these equations yield the decoupled ordinary differential equations (14) / (15) which describe *acoustic* and *advective* characteristics, respectively.

$$dp \pm \rho c \cdot du = [\pm c - (\gamma - 1)u]\,\mathcal{F} \quad on \quad dx/dt = u \pm c\,, \tag{14}$$

$$d\rho - \frac{1}{c^2}dp = \frac{(\gamma - 1)u}{c^2}\mathcal{F} \quad on \quad dx/dt = u\,. \tag{15}$$

It is worth pausing here to compare these equations and the liquid flow equations (8). The advective characteristic is new – it conveys information about the density in the system, which can change in gasses but not in liquids. The acoustic characteristics are, however, remarkably similar. The only differences are the modifying term on the right-hand side of the ordinary differential equations, and the differing positive and negative characteristic speeds. In fact, if the local velocity is zero, equation (14) is *exactly* equation (8).

3.3.2 Integration

For a gas, the density and sonic velocity cannot be considered fixed. Therefore, integrating equations (14-15) is no longer trivial. Nonetheless, the simplest approach is to *assume the thermodynamic quantities as fixed and again take the left Reimann sum*. It should be expected that this step may impart serious error when the flow is highly non-linear, and the calculation step is too large.

$$p_{new} = \underbrace{[p + (\pm c - (\gamma - 1)u)\mathcal{F} \cdot \Delta t \pm \rho c u]}_{C^{\pm}} \mp \underbrace{[\rho c]}_{B^{\pm}} u_{new} \quad on \quad dx/dt = \pm c \tag{16}$$

$$\rho_{new} = \underbrace{\left[\rho + \frac{(\gamma - 1)u}{c^2}\mathcal{F} - \frac{1}{c^2}p\right]}_{C_P} + \underbrace{\left[\frac{1}{c^2}\right]}_{B_P} p_{new} \tag{17}$$

Despite there being three equations (16-17) and three unknowns, the two acoustic characteristics are solved independently of the advective characteristic, and the results of this solution are used to find a new value for density.

3.3.3 Discrete solution

For gas flow, the local velocity and sonic velocity change as a particle moves along the characteristic, causing the path to curve. However, evaluating the integrals with a left Riemann sum implicitly assumes the characteristic speed over the finite path of integration is constant – approximating the characteristics to be straight lines as shown in Figure 2.

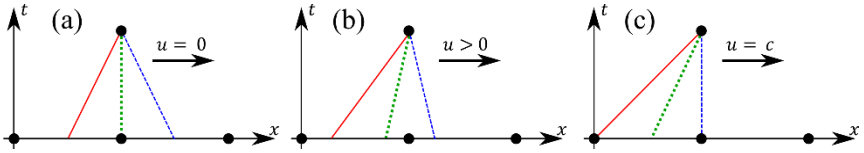

Figure 2: Characteristics at (a) zero flow (b) positive flow (c) Mach 1

The characteristics are symmetric only for stagnant flow (Figure 2a). As velocity increases, all three characteristics will tilt in the direction of flow (Figure 2b), and at a Mach number of 1, the downwind characteristic will be vertical (Figure 2c), indicating that no information can flow against the stream. In supersonic flow, all three characteristics have a slope of the same sign.

Unlike in Figure 1, the gas characteristic lines of Figure 2 do not intersect a prior node. A variation of properties between the nodes must be assumed to determine the conditions at the base of the characteristic. A simple *linear interpolation profile* is chosen here. While a linear interpolation does not have a high order of accuracy, unstable behavior is less likely [17]. Complex interpolations are certainly possible, though more care must be taken in selecting an appropriate scheme.

3.3.4 General junctions and boundary conditions

Just as for liquid flow, the availability of linear and explicit compatibility equations (18) makes the handling of complex inline junctions straightforward. The equations make it possible to capture nearly any behavior in a junction. Iterative routines are often more complex than in liquid flow, but the fundamental idea is the same.

$$p = C^{\pm} \mp B^{\pm}u \qquad \rho = C_P + B_P p \tag{18}$$

A branching-type junction can also utilize these equations. For example, a simple branch with no losses must have a single stagnation pressure and density at the common point of connection. A trial pressure and density can be asserted at the common point, and the compatibility equations for all connections can be evaluated in turn. This evaluation may indicate an imbalance in conservation of mass or energy around the branch. This discrepancy can be used to appropriately adjust the trial pressure and density up or down, driving it to a correct value via iteration.

4 THE FINITE VOLUME METHOD

4.1 Overview

The Finite Volume Method (FVM) *enforces* [18] conservation in the hyperbolic system via integration of equation (3) over a finite control volume. It is easy to understand that for some arbitrary volume without a source term, the net amount of conserved quantity entering the volume must cause an equal increase in said quantity within the volume. Adopting a careful approach in applying this integration numerically ensures conservation for every volume in the model.

4.1.1 Some advantages of the FVM

Most modern general flow analysis research seems focused on the FVM. It is fair to state that it is strongly preferred for general flow analysis, perhaps because of the strict enforcement of conservation laws, which is an extremely desirable trait. It is also general enough in concept to allow for the inclusion of a dramatic range of effects, such as electromagnetic or even relativistic effects [19]. A properly implemented scheme that accounts for all pertinent physical effects will approach the true solution as the computational element count increases.

An assumption made in forming the differential system of equations (4) was that the behavior of the conserved variables is *smooth*. If the behavior is not smooth, a required step in transforming the integral(s) (3) into the differential equation(s) (4) is not valid. Therefore, the differential form cannot be solved for if a property has a jump discontinuity. A central advantage of the FVM is the use of the more fundamental integral form, which does not rule out the presence of discontinuities in properties.

4.1.2 Some disadvantages of the FVM

Discrete numerical solutions require approximation of some kind - most FVM analyses utilizing fewer computational volumes will still be inaccurate, even while the masses, momentums, and energies in a cell are conserved. To offset this, using more computational volumes runs the risk of becoming computationally time-consuming – especially for high-order accurate, multi-dimensional, or multi-physical FVM schemes. It is a fair assessment to extend this line of thinking to large piping systems.

The FVM nominally "stores" volume-averaged cell values at a location within the cell but requires intercell fluxes to update these values. These fluxes are not necessarily straightforward to compute and often require a method for approximating properties at intercell locations, introducing computational error. The methods to compute these fluxes are commonly known, but many flux schemes have a variety of strengths and weaknesses [9]. This typically makes FVM methods more advantageous on a case-by-case basis, rather than within a generalized scope.

A robust FVM tends to be significantly more complicated [8] [9] than the MOC formulation presented in section 3. These complexities make the development of sophisticated boundaries much more nuanced than the comparable MOC solution. While FVM excels at implementing known value or known flux boundaries, the implementation of junction-style boundary conditions (such as valves or pumps) is more complex. These types of boundaries require conditionally known properties at the intercell location rather than at the internal node. For the FVM, this would require approximation and iteration.

4.2 A common approach

This paper is not intended to cover in detail the many possible FVM variations – many excellent resources exist to that end [8] [9] [18] [19]. Instead, we discuss the foundations of a common approach in modern codes. The goal is to describe a high-resolution scheme that is computationally efficient, captures shocks, handles source terms, and allows for complex boundaries.

Stated briefly, a usual approach is to use some type of *Reconstruct, Evolve, Average* algorithm [8] [9]. The *reconstruction* step involves determining an approximate variation of properties within a particular computational cell from the previous step results. The *evolution* step uses the reconstructed profile to determine the intercell fluxes and moves, or evolves, the profile accordingly. Finally, the *average* step determines new cell-averaged values from the evolved profile for use in the next time step.

4.2.1 Options for reconstruction

The simplest approach is to assume that values within computation cells prevail throughout the cell volume, which results in a *piecewise-constant* variation of the conserved properties along the computational domain. The Godunov method, which "revolutionized the field of computational fluid dynamics" [8, p. 77], uses a piecewise-constant profile as one of its building blocks, which limits the accuracy that can be attained [9].

The next simplest option is to assume a *piecewise-linear* variation within each cell, which can improve the overall method to second-order accuracy. The linear profile is chosen to be upstream centered, a component of the MUSCL (Monotonic Upstream-centered Scheme for Conservation Laws) scheme [20]. The current cell value and upstream cell value are assumed to define a slope *in the current cell*. It does not mean that a continuous variation throughout the domain is assumed – as with the piecewise-constant choice, there are still *discontinuities* at each cell interface.

To *evolve* this solution, the flux must be calculated at the interfaces. However, the discontinuities mean that the derivatives are infinite, and equation (3) cannot be used. Instead, a Riemann problem is solved at each interface.

4.2.2 Monotonicity, slope limiters, and Total Variation

Before solving the Riemann problem, we must address the fact that a piecewise-linear profile has the propensity to cause spurious oscillations in the solution near strong discontinuities in the flow. These oscillations are unphysical – a *monotonic* solution is desired.

An option to enforce monotonicity is to apply a *slope limiter*. Properly designed slope limiters conform to a condition known as Total Variation Diminishing (TVD) [8] [9]. This property enforces a physically reasonable constraint that the *variation* – pressure rise across a shock for example – must *diminish* with time, across the entire domain. Application of a TVD slope limiter is a key component of the MUSCL scheme.

4.2.3 The Riemann problem

The Riemann problem considers a system of conservation equations and specifies initial values which are constant except for a single discontinuity at the center of the domain. It is of particular interest because *exact solutions* can be found.
This problem is of great interest to the FVM because the reconstruction steps taken so far have generated a Riemann problem at every cell interface. Therefore, the questions of determining the intercell flux and solving the Riemann problem are effectively identical.

The *shock tube problem*, a famous test problem discussed by Sod [21], is an example of the Riemann problem for the Euler equations. In a typical case, the discontinuous initial values will generate a rarefaction wave, a contact discontinuity, and a shock, and this variety of conditions lends the problem value as a verification case.

It is interesting to note that the MOC is a key component in the exact solution of the Riemann problem. The characteristics in the system interact to help form a particular wave structure, but the MOC alone is not enough to solve the problem. When characteristics of the same family converge, a shock is formed, which requires application of the Rankine-Hugoniot conditions. When they diverge, a rarefaction or expansion fan is generated, and isentropic relations are needed. The Riemann problem can be solved exactly, but the solution does not have a closed form, so computationally expensive iteration is required.

4.2.3.1 Approximate Riemann solvers

It is obvious that the true variation of properties along the domain is not piecewise-constant, nor piecewise-linear, and this estimation will impart error. It is not generally worth the effort of procuring an exact solution to a Riemann problem based on approximate data. Instead, an approximate solver can be used, which attempts to estimate with some reasonable degree of accuracy the solution structure, *without iteration*.

One such approximate solver is HLLC (Harten-Lax-van Leer-Contact) [22], which uses an estimated pressure to approximate the highest characteristic speed in both directions, estimates the speed of the advection wave, and then estimates the flux at the interface.

4.2.4 Handling source terms

Attempting to solve the system of partial differential equations with source terms directly is quite difficult. Instead, this problem can be split into two simpler sub-problems, in what is known as a *fractional-step* approach [8] [9]. The homogenous (no source terms) problem is solved as above. Then, the *result* of that solution is used as an initial condition for the *ordinary* differential equation based on the source terms, which when solved gives the values for the new time level.

This approach is only first order accurate, and it may introduce *splitting error* if the operations are not commutative. A second order accurate approach is to take a half-step application of the source term ordinary differential equation before and after the full step homogeneous solution [9].

4.2.5 General junctions and boundary conditions

A typical approach to boundaries in the FVM is to define ghost cells (additional computation cells outside of the physical domain). The ghost cell conditions are modified at the beginning of a step to create the intended conditions at the boundary face. This process is significantly more difficult when trying to model devices like centrifugal compressors or valves.

The authors know from first-hand experience that attempting *analytic* solutions for even "simple" junctions like a valve is exceedingly complicated even with the MOC compatibility equations. Developing such solutions for a wide variety of junctions may be theoretically possible, but it would be very impractical. Instead, for both FVM and MOC, the authors suggest focusing on iterative techniques.

5 EXAMPLES

5.1 Low shock strength ideal shock tube

This problem considers a perfect gas ($\gamma = 1.4$) without friction. The dimensionless system has a length of 1, and a discontinuity at 0.5. The initial conditions are: $\rho_L = 1, u_L = 0, p_L = 1, \rho_R = 0.125, u_R = 0, p_R = 0.2$. The CFL number for MOC application is approximately 0.9. The results are presented at time 0.2.

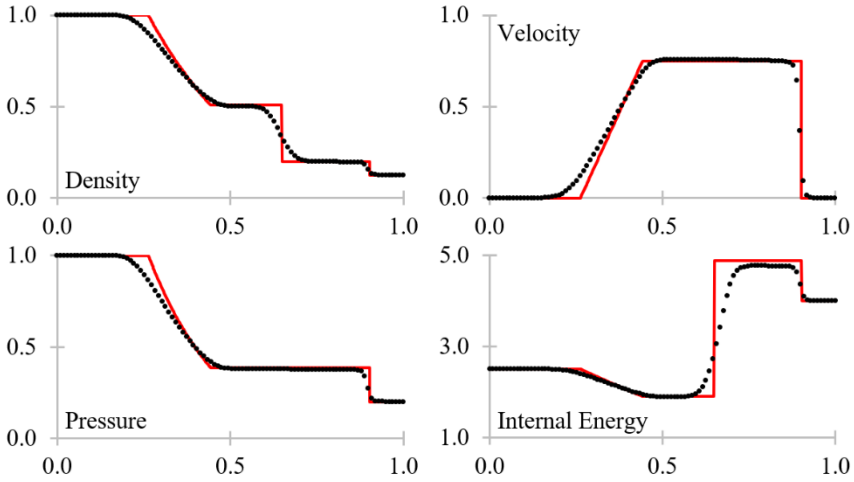

Figure 3: Low shock strength. Exact (solid) and 100 node MOC (dots).

Figure 3 shows the exact results compared against the MOC with 100 nodes. The MOC results are not exact, but they are what many would consider accurate for practical purposes. Figure 4 shows the effect of varying node count at the shock front and at the contact discontinuity. As expected, adding more nodes makes the solution approach the true values.

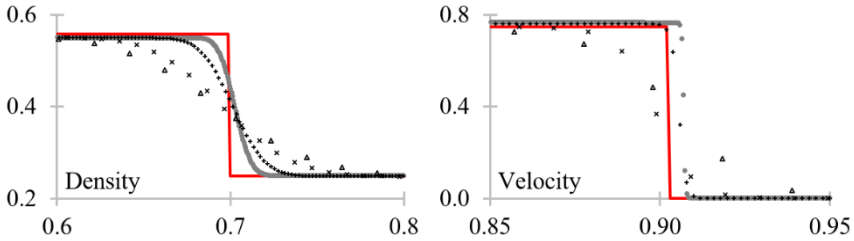

Figure 4: Effect of varying MOC node count on the contact discontinuity and shock. Exact (solid), 50 (triangle), 100 (cross), 500 (plus), 2000 (dot)

5.2 Moderate shock strength ideal shock tube

This example is identical to the previous example except that p_R has been lowered to 0.1. This represents the original Sod shock tube problem [21]. Figure 5 shows exact results, MOC results, and the Godunov method applied with a Roe approximate Riemann solver [22]. Both the MOC and FVM results were determined with 200 nodes.

The MOC seems to do reasonably well, except for the internal energy prediction, which the authors believe is due primarily to the MOC formulation presented not having any specific features for shock capturing. One textbook author specifically refers to this weakness with a note that a "moderate shock pressure ratio of 4.08" gives results that are within "reasonable accuracy for many engineering applications" (Moody, [11, p. 459]).

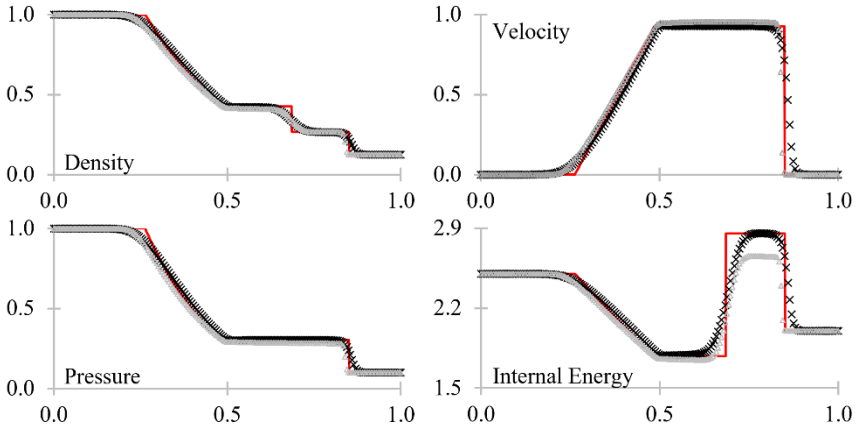

Figure 5: Moderate shock strength. Exact (solid), MOC (light triangle), Godunov (dark cross)

In investigating this discrepancy, the authors found increasing conservation error across the shock with increasing shock strength. The Riemann problem, used for the analytic solution of the shock tube problem, specifically incorporates the Rankine-Hugoniot conditions that enforce conservation across the shock. The MOC as described here does not enforce these conditions, so it is not surprising that they are not met. Figure 6 shows the relationship between the pressure ratio p_L/p_R and percentage loss of conserved properties across the shock. Note that this test was carried out by modifying only p_R, with all other values as indicated by the prior example.

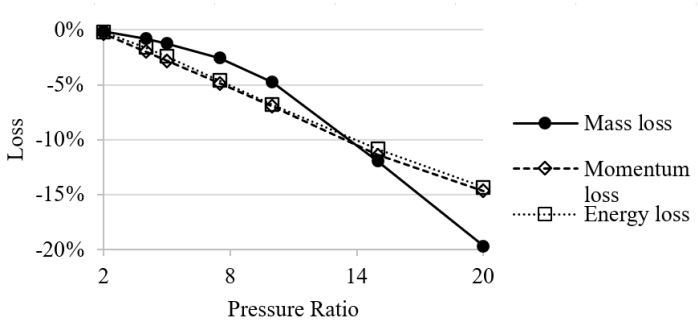

Figure 6: Conservation loss across shock vs. shock tube pressure ratio in the MOC

5.3 Steady choked flow

It is perhaps most intuitive to understand the conservation problems with the MOC when observing a steady simulation. It is expected that mass and energy flow into and out of an adiabatic pipe are equal. The results in Figure 7 were generated with a hydraulically smooth 30 m pipe of 10 cm internal diameter, an inflow of 10 kg/sec at 300 °C, discharging to atmospheric pressure. The fluid is steam with a Redlich-Kwong EOS. The analytic results were determined with AFT Arrow [23], a steady-state tool which enforces conservation explicitly, and the MOC results were determined with AFT xStream [23], an unsteady tool based on the MOC formulation described in this paper.

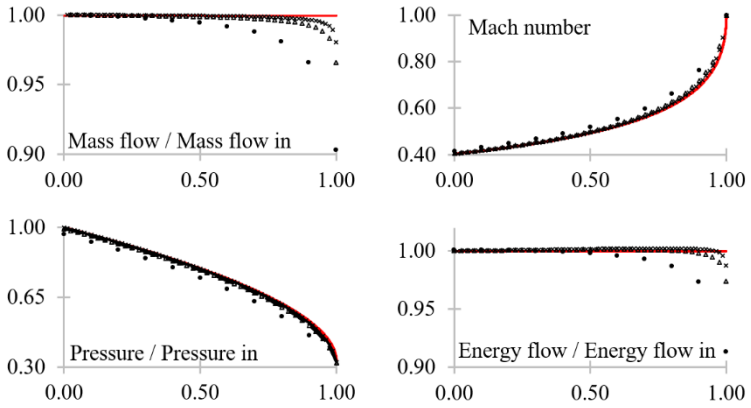

Figure 7: Steady-state choked flow, actual and MOC results. Exact (solid), 11 nodes (dots), 41 nodes (triangles), 81 nodes (crosses).

The MOC is reporting an unexpected mass and energy flow loss down the pipe – this is due to the estimations imparted by the profile assumption and numeric integration [24]. The non-linear velocity profile is the primary cause, as the finite characteristic lines are unaware of the increase in velocity over their length. As the segments are made smaller, the non-linear effects become smaller and therefore the approximation becomes more accurate. This example considers choked flow, a situation that will naturally exacerbate these problems. For sensitive and exacting applications, these results may not be acceptable. But for a typical network-level analysis, these results are generally satisfactory – the small error here is unlikely to impact any design decisions made.

5.4 A shock tube with friction

This example is similar in structure to the low shock strength problem investigated in section 5.1 but includes the effect of friction using the Darcy-Weisbach and Colebrook-White equations. The system is no longer dimensionless. We consider a perfect gas in a pipeline of length 2000 m with a discontinuity at 1000 m. Initial conditions are $\rho_L = 1\,\mathrm{kg/m^3}$, $u_L = 0\,\mathrm{m/s}$, $p_L = 1\,\mathrm{bar}$, $\rho_R = 0.125\,\mathrm{kg/m^3}$, $u_R = 0\,\mathrm{m/s}$, and $p_R = 0.2\,\mathrm{bar}$ – creating the same dimensionless ratios as section 5.1. For friction calculations, we consider the pipe diameter $D = 10.22\,\mathrm{cm}$ and absolute roughness $\epsilon = 4.571 \times 10^{-3}\,\mathrm{cm}$.

The results were generated at the times of 0.2 and 1 seconds with a count of 200 computational nodes for both the MOC and FVM. The MOC results were generated with AFT xStream [23], while the FVM results were generated with an in-house validated program. The in-house program uses a Godunov scheme and a second-order fractional-step method (see section 4.2.4) to update the conserved

variables to the following computational time. The source term (friction) is computed with a 2nd order Runge-Kutta method while intercell fluxes are approximated with the Roe method (see section 4.2.3.1).

Figure 8 compares the static pressure and velocity results between the MOC and FVM methods. The comparative results align well throughout the length of the tube. The FVM scheme implies the wave has traveled slightly faster downstream in comparison to the MOC scheme in both the 0.2 second and 1 second snapshots. This is likely due to the MOC struggling to preserve information across shocks at higher Mach numbers – the discontinuity reaches $Ma \approx 0.6$ at the beginning of the simulation, which would cause the MOC to lose a small amount of conserved property information early in the simulation, but the effects do not worsen with time.

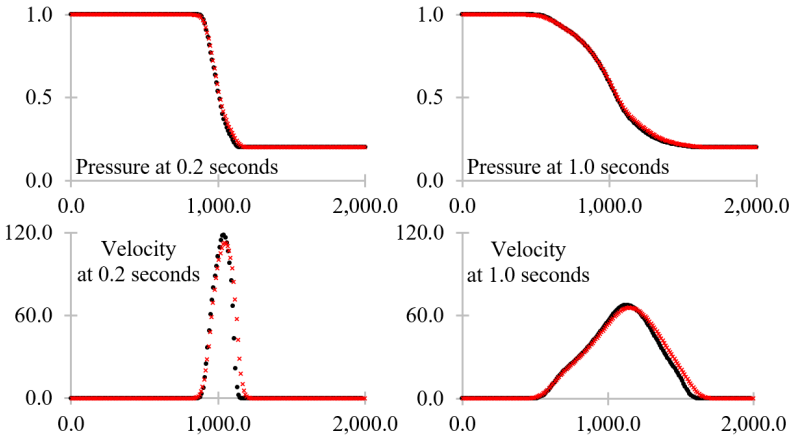

Figure 8: Friction shock tube comparison. MOC (dots) and FVM (crosses). Pressure in bar, velocity in meters per second, and length in meters.

6 CONCLUSIONS AND FUTURE WORK

The MOC as a tool will never replace FVM, which excels in both accuracy and flexibility. However, industrial tools must consider practicality of both development of tools and their use. To that end, the authors believe the tests shown here demonstrate that the MOC is worthy of consideration for the analysis of unsteady compressible transients under some conditions and should be considered a valuable piece of the engineer's toolkit.

The authors intend to investigate further the effects of real gasses, source terms, and complex boundaries in both solution methods. The present work was intended primarily to show that the MOC is a viable option for the analysis of compressible flow in piping networks, and therefore focused on relatively simple test cases. The authors believe the method shows promise, and that further research is warranted.

Like the FVM, future investigations could result in vast improvements in simulation quality. The simplest FVM formulations often have results that are very inaccurate, while complex schemes can make them some of the most accurate tools available. The authors believe it is reasonable to assume that with dedicated research effort, dramatic improvements to the MOC are possible, building on results that are already practically actionable in many engineering contexts.

7 REFERENCES

[1] B. E. Wylie and V. L. Streeter, Fluid Transients in Systems, Upper Saddle River, NJ: Prentice Hall, 1993.

[2] A. R. D. Thorley, Fluid Transients in Pipeline Systems, Second Edition, Professional Engineering Publishing Limited, 2004.

[3] A. Majumdar, A. LeClair, R. Moore and P. Schallhorn, "Generalized Fluid System Simulation Program, V6," NASA Marshall Space Flight Center, 2016.

[4] H. Goyder, "Gas Waterhammer," in *PVP2007*, San Antonio, Texas, 2007.

[5] A. R. D. Thorley and C. H. Tiley, "Unsteady and transient flow of compressible fluids in pipelines - a review of theoretical and some experimental studies," *International Journal of Heat and Fluid Flow,* vol. 8, 1987.

[6] T. W. Walters, G. G. Orieux, Q. Li and L. Thomson, "Making the world a safer and better place - a plea for more data, validation cases and guidelines for waterhammer simulation," in *Pressure Surges 13*, 2018.

[7] A. Vardy and Z. Pan, "Quasi-steady Friction in Transient Polytropic Flow," *Computers & Fluids,* vol. 26, no. 8, pp. 793-809, 1997.

[8] R. J. LeVeque, Finite Volume Methods for Hyperbolic Problems, Cambridge University Press, 2002.

[9] E. F. Toro, Riemann Solvers and Numerical Methods for Fluid Dynamics: A Practical Introduction, 3 ed., Heidelberg: Springer Berlin, Heidelberg, 2009.
[10] J. M. Smith and H. C. Van Ness, Introduction to Chemical Engineering Thermodynamics, Fourth Edition, McGraw-Hill, 1987.
[11] F. J. Moody, Intro. to Unsteady Thermofluid Mechanics, John Wiley & Sons, 1990.
[12] A. Khamoushi, A. Keramat and A. Majd, "One-Dimensional Simulation of Transient Flows in Non-Newtonian Fluids," *J. of Pipeline Systems Engineering and Practice,* vol. 11, no. 3, 2020.
[13] S. Henclik, "A Numerical Approach to the Standard Model of Water Hammer with Fluid-Structure Interaction," *J. of Theoretical and Applied Mechanics,* vol. 53, 2015.
[14] A. Adamkowski and M. Lewandowski, "Experimental Examination of Unsteady Friction Models for Transient Pipe Flow Simulation," *J. of Fluids Engineering,* vol. 128, 2006.
[15] W. Meng and e. al., "GPU Acceleration of Hydraulic Transient Simulations of Large-Scale Water Supply Systems," *Applied Sciences,* vol. 9, no. 91, 2018.
[16] C. P. Liou and E. B. Wylie, "Approximation of the Friction Integral in Water Hammer Equations," *Journal of Hydraulic Engineering,* vol. 140, no. 5, 2014.
[17] A. Vardy and Z. Pan, "Numerical accuracy in unsteady compressible flows," in *Pressure Surges*, 2000.
[18] S. V. Patankar, "Numerical Heat Transfer and Fluid Flow," Hemisphere Publishing Corporation, 1980.
[19] M. F., M. L. and D. M., The Finite Volume Method in Computational Fluid Dynamics, Springer International Publishing Switzerland, 2016.
[20] B. van Leer, "MUSCL, A New Approach to Numerical Gas Dynamics," in *Second European Conference on Computational Physics*, Garching, 1976.
[21] G. A. Sod, "A Survey of Several Finite Difference Methods for Systems of Nonlinear Hyperbolic Conservation Laws," *J. of Comp. Physics,* vol. 27, 1978.
[22] E. F. S. M. S. W. Toro, "Restoration of the Contact Surface in the HLL-Riemann solver," *Shock Waves,* vol. 4, pp. 25-34, 1994.
[23] Applied Flow Technology, *AFT Arrow & AFT xStream software tools,* Colorado Springs, CO: www.aft.com, 2023.
[24] A. E. Vardy, "Method of characteristics in quasi-steady compressible flows," in *Pressure Surges 10*, 2008.